# Multiphoton radiofrequency resonances in $He_4^+$ †

J. R. Brandenberger,* S. R. Lundeen, and F. M. Pipkin
*Lyman Laboratory of Physics, Harvard University, Cambridge, Massachusetts 02138*
(Received 9 February 1976)

One-, two-, three-, and four-photon resonances in the $N = 6$, 7, and 9 states of $He_4^+$ have been observed with a fast atomic beam. The locations, amplitudes, widths, and rf Stark shifts of these resonances are discussed along with the prospects for exploiting multiphoton fast-beam spectroscopy as a means for measuring the fine structure of $He_4^+$ to high precision.

Multiphoton rf spectroscopy provides a new technique for measuring fine-structure splittings, the fine-structure constant, and radiative corrections to hydrogenic atoms.[1] To better assess the potential of this method, we have used it to measure several splittings in $He_4^+$ where the fine structure is unencumbered by hyperfine effects and remains largely unexplored. The present paper reports the first observation of two-, three-, and four-quantum resonances in $He_4^+$ and describes the basic properties of these resonances. It is shown that the positions, sizes, and shapes of these resonances are in agreement with the predictions of a simple, approximate treatment of the multiphoton line shape.

When an atom is subjected to a strong rf electric field, its temporal evolution can be described by the semiclassical perturbing Hamiltonian

$$\mathcal{H}' = e\vec{\mathcal{E}} \cdot \vec{r} \cos\omega t .$$

Shirley[2] has shown that the dynamics of such a system can be described by an infinite but static "Floquet" Hamiltonian $\mathcal{H}_F$ whose basis states $|\alpha, p\rangle$ are labeled by the usual atomic quantum numbers $\alpha$ and an additional integer $p$. These states are interpretable as product states of the atomic system and a quantized rf field with mean photon number $N+p$ where $N \gg 1$. $\mathcal{H}_F$ has diagonal elements

$$\langle \alpha, p | \mathcal{H}_F | \alpha, p \rangle = E_\alpha + p\hbar\omega$$

and off-diagonal elements

$$\langle \alpha, p | \mathcal{H}_F | \beta, p \pm 1 \rangle = \tfrac{1}{2} e\vec{\mathcal{E}} \cdot \langle \alpha | \vec{r} | \beta \rangle .$$

When the rf frequency $\omega$ is such that the states $|\alpha, p\rangle$ and $|\beta, p \pm n\rangle$ are nearly degenerate, an $n$-quantum transition becomes possible providing the resonant levels are coupled *in any order*. Diagonalization of $\mathcal{H}_F$ in this region reveals an "anticrossing" of the Floquet eigenvalues and a resonant behavior in the atomic transition probabilities that can be described by this procedure to arbitrary precision.

In cases where the anticrossed states are well isolated in energy from the other Floquet states, an adequate description of the resonance can be obtained from an effective two-level Hamiltonian[3]

$$\mathcal{H}_{\text{eff}} = h \begin{bmatrix} \nu_\alpha + \Delta\nu_\alpha & V_{\alpha\beta} \\ V_{\alpha\beta} & \nu_\beta + \Delta\nu_\beta + n\nu \end{bmatrix},$$

where $\Delta\nu_\alpha$ and $\Delta\nu_\beta$ represent shifts in the energies of the states produced by nonresonant interaction with distant Floquet states, and $V_{\alpha\beta}$ is the lowest-order coupling between the resonant levels. Near a resonance, $\Delta\nu_\alpha$, $\Delta\nu_\beta$, and $V_{\alpha\beta}$ can be evaluated in terms of the rf field $\mathcal{E}$ using elementary time-independent perturbation theory. If we assume that an rf field of uniform amplitude is applied for a time $T$, and that the radiative lifetimes of the resonant levels are negligible on this time scale, the atomic transition probability is given by

$$P_{\alpha\to\beta}(T) = (|V_{\alpha\beta}|^2/q^2) \sin^2 2\pi q T , \tag{1}$$

where

$$q^2 = |V_{\alpha\beta}|^2 + \tfrac{1}{4}(n\nu - \nu_0^*)^2 ,$$

$$\nu_0^* = (\nu_\alpha + \Delta\nu_\alpha) - (\nu_\beta + \Delta\nu_\beta) .$$

The observations reported here were obtained with the apparatus of Fig. 1. $He^{++}$ ions, accelerated through 80 kV, pass through a differentially pumped gas target to emerge as fast excited $He^+$ ions. After traversing a short drift region, the ions pass through a parallel-plate capacitor across which is applied an rf electric field with peak amplitude of 0–20 V/cm. The rf capacitor is matched to and inserted into a 50-Ω transmission line so that the rf amplitude may be inferred from the power transmitted through the plates. After

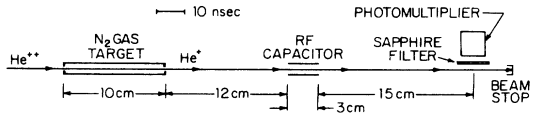


FIG. 1. Experimental arrangement.

emerging from the capacitor, the ions pass in front of a solar blind vacuum ultraviolet photomultiplier which monitors the rate of 1640-Å Balmer-$\alpha$ emission from the $He^+$ ions. rf-induced transitions change the excited state populations in the beam, and will, in general, change the photocurrent. (The size and sign of that change depend on the lifetimes and branching ratios of the particular states involved.) Since the 1640-Å photon is a cascade decay product of many excited $He^+$ states, transitions involving these states may be detected in the photocurrent. The experimental signal is defined as the fractional decrease in the photocurrent level produced by turning on the rf field.

Figure 2 shows the rf signals obtained in the frequency range 600–940 MHz at several different rf field amplitudes. The five resonant features are identified in Table I. Note that at weak rf fields the single- and double-photon resonances dominate the spectra, but that with stronger fields higher-order resonances occur with comparable strength. Particularly evident in Fig. 2 are the strong rf Stark shifts in the resonance positions. Experimental limitations precluded full examination of resonance 1 at fields exceeding several V/cm. To extract the characteristic features of the five resonances from the data of Fig. 2, a function consisting of five separate Lorentzians (alternately Gaussians) and a constant background was least-squares fitted to the data. Up to 15 parameters were floated simultaneously to determine the positions, widths, and amplitudes of the separate resonance complexes. The solid lines in Fig. 2 represent fitted Lorentzian composites, though Gaussian line shapes fit equally well.

The center frequencies obtained from the fits were used to determine both the zero-field fine structure and the shift rates. Diagonalizations of $\mathcal{H}_F$, using theoretical fine-structure intervals, indicated that the shifts should be approximately linear in the square of the rf field, but that higher-order terms ($\mathcal{E}^4$, etc.) should begin to contribute at the highest field strengths used. Since the precision of the present data precluded testing of the higher-order terms, the experimental center frequencies $\nu_0(\mathcal{E})$ were extrapolated to zero field strength by fitting to the function

$$\nu_0(\mathcal{E}) = \nu_0(0) + k\mathcal{E}^2 . \tag{2}$$

Although the resulting intercepts $\nu_0(0)$ are approximately equal to the zero-field fine-structure intervals, small errors could be introduced through the use of Eq. (2). To correct for these errors, the following procedure was followed: Theoretical center frequencies $\nu_0(\mathcal{E})$, calculated at the same values of $\mathcal{E}$ for which experimental center frequencies existed, were also fitted to Eq. (2). The differences $\delta\nu$ between the resulting $\nu_0(0)$'s and the theoretical zero-field fine-structure intervals (initially input to the calculation) represent a measure of the approximations inherent in Eq. (2). Assuming that the experimental and theoretical extrapolations behave in the same manner, the $\delta\nu$'s were added to the experimental $\nu_0(0)$'s to obtain our best estimate of the zero-field fine-structure intervals. The results are collected in Table I. The experimental fine-structure intervals (column 6) are in excellent agreement with the calcu-

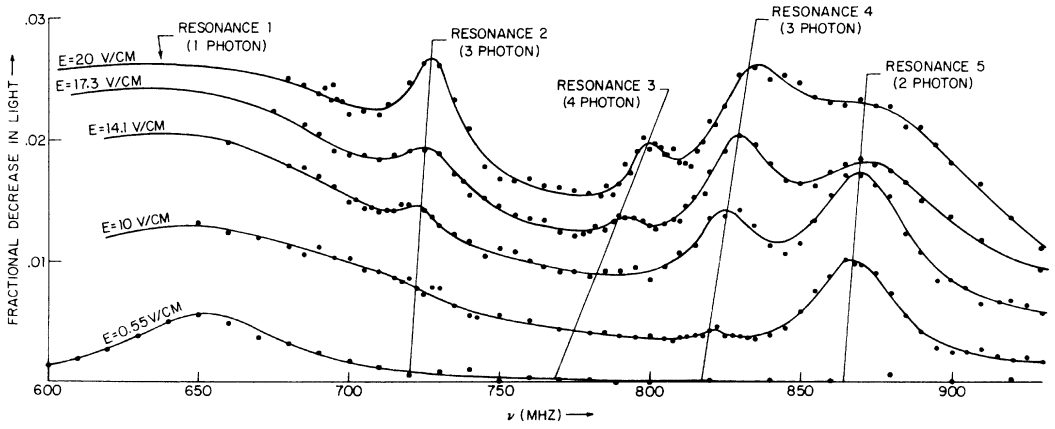


FIG. 2. Multiphoton spectra showing the five resonant features identified in Table I. Solid curves represent composite theoretical line shapes fitted to the experimental data points. One standard deviation for each point corresponds to approximately two diameters of the plotted points. The straight lines indicate the shifts of the resonances with rf power.

TABLE I. Observed resonances and results of present work. The frequencies in column 4 represent $1/n$ of the total theoretical splittings, while the frequencies in column 5 are weighted averages over the components in each resonant complex. Column 6 includes the experimentally determined zero-field fine structure derived from the extrapolation procedure described in the text. Columns 8 and 9 compare calculated and measured rf Stark shifts.

| Resonance | Number of photons | Transition | $\nu_{\text{theory}}$ (MHz) | Weighted $\nu_{\text{theory}}$ (MHz) | $\nu_{\text{expt}}$ (MHz) | $\delta\nu$ (MHz) | Theoretical shift rate (MHz cm$^2$/V$^2$) | Experimental shift rate (MHz cm$^2$/V$^2$) |
|---|---|---|---|---|---|---|---|---|
| 1 | 1 | $6F_{7/2}$-$6G_{9/2}$<br>$6G_{7/2}$-$6H_{9/2}$ | 648.21(9)<br>649.00(3) | 648.80(20) | | | | |
| 2 | 3 | $6D_{5/2}$-$6H_{11/2}$ | 720.10(4) | 720.10(4) | 720.4(10) | +0.08 | 0.017(8) | 0.020(2) |
| 3 | 4 | $9P_{1/2}$-$9H_{9/2}$ | 769.37(4) | 769.37(4) | 774.3(40) | +2.16 | 0.074(2) | 0.068(11) |
| 4 | 3 | $7P_{3/2}$-$7G_{9/2}$<br>$7D_{3/2}$-$7H_{9/2}$ | 815.42(2)<br>817.48(3) | 816.97(51) | 817.6(12) | +0.03 | 0.036(2) | 0.039(4) |
| 5 | 2 | $6D_{5/2}$-$6G_{9/2}$<br>$6F_{5/2}$-$6H_{9/2}$ | 864.02(6)<br>865.36(4) | 865.03(34) | 864.3(7) | −0.32 | 0.024(3) | 0.027(3) |

lations of Erickson,[4] as represented by columns 4 and 5 of Table I. The errors shown in column 6 are statistical only and do not include a systematic uncertainty estimated to be ±1 MHz.

The fits of both the experimental and theoretical center frequencies to Eq. (2) also provided a test of the shift calculations. The excellent agreement between the shift coefficients $k$ in columns 8 and 9 indicates that the Floquet formalism is able to describe these rf Stark shifts from first principles.

The fits to the spectra of Fig. 1 also yielded information on the amplitudes and widths of the individual resonances. To the extent that the natural widths of the resonances are negligible,[5] Eq. (1) suggests that the amplitudes and widths should scale as a simple function of the average effective coupling strength $\bar{V}_{\alpha\beta}$ for each resonance. Both curves in Fig. 3 are consistent with these relationships implied by Eq. (1) if one assumes an effective transit time $T$ through the rf plates of 14 nsec.[6] Of course a more rigorous description of the resonant line shape must take account of the approximations underlying Eq. (1).

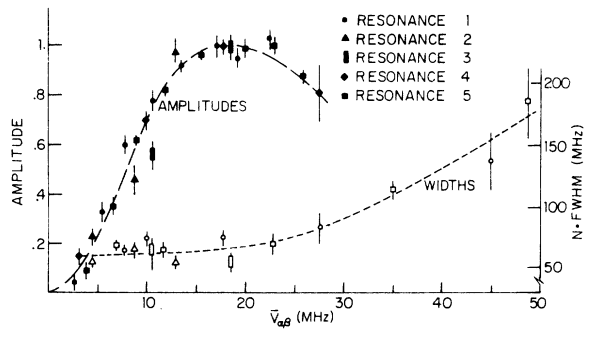


FIG. 3. Normalized relative amplitudes and $n\times$ (full width at half-maximum)of five resonances as a function of the average coupling strength $\bar{V}_{\alpha\beta}$ for each complex.

Of the resonances studied here, only resonance 3 consists of a single component. Resonance 2 is a superposition of three simple resonances ($|M_J| = |M'_J| = \frac{1}{2}$, $\frac{3}{2}$, and $\frac{5}{2}$), each of which shifts at a different rate, though all extrapolate to the same zero-field interval. Resonances 1, 4, and 5 add a second complication, a near degeneracy between resonances corresponding to different $L$ values. In all cases, the relative weights of the various simple resonances in the superposition are poorly understood, fundamentally owing to uncertainty in the $M_J$ and $L$ dependence of charge exchange cross sections. These complications are the major cause of the theoretical uncertainties in columns 5 and 8 of Table I.

The measured fine-structure intervals shown in Table I do not by any means represent the full potential of this technique for precision work. The real advantage of the multiquantum technique in the study of hydrogenic fine structures is the availability of transitions of very high $Q$ [(transition frequency)/(natural width)]. The three-quantum $4S_{1/2}$-$4F_{7/2}$ transition, for example, has a natural $Q = 1350$ and consists of a single component that would be free of complications due to multiple lines. These facts suggest that this interval might be measured to a few parts in $10^7$ by this technique. Such a measurement could be used to obtain the radiative shift of the $4S_{1/2}$ level in $He_4^+$ with a precision considerably greater than that presently available in any hydrogenic system.

†Research supported by the National Science Foundation under Grant MPS74-13728.

*Permanent address: Lawrence University, Appleton, Wisc. 54911.

[1]P. B. Kramer, S. R. Lundeen, B. O. Clark, and F. M. Pipkin, Phys. Rev. Lett. 32, 635 (1974).

[2]J. H. Shirley, Phys. Rev. 138, B979 (1965).

[3]H. Salwen, Phys. Rev. 99, 1274 (1955).

[4]G. W. Erickson (private communication).

[5]Other broadening mechanisms include power broadening and transit-time broadening due to short interaction times $T$ during which the rf field is active. These mechanisms are predominant in the present work.

[6]Although the ions remain within the physical dimensions of the capacitor for only 11 nsec, fringing of the rf fields is sufficient to lengthen the effective transit time to about 14 nsec.